2003

Calculation of the temperature dependent AC susceptibility of superconducting disks

M. J. Qin
University of Wollongong, qin@uow.edu.au

G. Li
University of Wollongong

Hua-Kun Liu
University of Wollongong, hua@uow.edu.au

S. X. Dou
University of Wollongong, shi@uow.edu.au

Calculation of the Temperature Dependent AC Susceptibility of Superconducting Disks

M. J. Qin, G. Li, H. K. Liu, and S. X. Dou

***Abstract*—The temperature dependent complex AC susceptibilities of high temperature superconducting disks in perpendicular AC magnetic fields (in absence of DC magnetic field) have been calculated from first principles. The temperature dependent AC susceptibilities for different AC field amplitudes, AC field frequencies, reduced pinning potential, and sample thickness have been derived, which demonstrate many features different from what has been observed in the configuration of infinite long slab or cylinder under a parallel-applied AC field. The results of such a realistic configuration of finite-thickness samples in perpendicular fields can be compared directly to the experimental results.**

***Index Terms*—AC susceptibility, high temperature superconductor, perpendicular and parallel field, pinning potential.**

I. Introduction

AC magnetic measurements have been widely used to study the magnetic properties and flux dynamics of superconductors [1]–[18]. The advantage of using magnetic measurement over transport measurement is that magnetic measurement is contact-less. AC magnetic measurements are usually more sensitive than DC magnetic measurements because phase sensitive detector can be used to achieve higher sensitivity.

However, the analysis of the results from magnetic measurements is usually more difficult than transport measurements because the magnetic field profiles of the sample are needed to calculate the current density, especially when samples are mounted perpendicularly to the applied magnetic fields, which is the usual case in the measurements. Analytically, such a perpendicular configuration is difficult to analyze, because of the extreme demagnetization effect. Present models used to account for the results of AC measurements [11], [14]–[17] are usually based on infinite long slab or cylinder immersed in a parallel-applied magnetic field.

The magnetic properties of the superconductor under perpendicular magnetic field have been intensively studied in recent years. Analytical results have been derived for samples with zero thickness. Recently, Brandt has developed a new method from first principles to calculate the magnetic response of superconducting strips and disks with finite thickness under perpendicular field [19]–[24]. Magnetization hysteresis loops, AC susceptibility, detailed field and current distribution with or without transport current, surface and geometric barrier have been studied by Brandt. AC susceptibility as a function of AC field amplitude has also been presented. However, experimentally AC susceptibility is usually measured as a function of temperature. In this paper, the current and field profiles of superconducting disks under perpendicular field are derived, and AC susceptibility is calculated as a function of temperature for different AC field amplitudes, frequencies and pinning potentials. The results can be compared directly to the experimental results.

Manuscript received August 5, 2002. This work was supported by the Australian Research Council.

The authors are with the Institute for Superconducting and Electric Materials, University of Wollongong, Wollongong, NSW 2522, Australia (e-mail: qin@uow.edu.au; gl05@uow.edu.au; hua_liu@uow.edu.au; shi_dou@uow.edu.au).

Digital Object Identifier 10.1109/TASC.2003.812537

II. Calculation Method

We consider a superconducting disk with radius a and thickness $2b$ in an AC field of $H(t) = H_{\rm ac}\sin(\omega t)$ applied parallel to the disk axis along y. Because of the axial symmetry of the problem, only the quarter cross-section $0 \le r \le a$, $0 \le y \le b$ is considered. We use cylindrical coordinate system (r, ϕ, y), with y along the symmetrical axis, and r parallel to the surface of the disk. In this case the current density $\boldsymbol{J}$, electric field $\boldsymbol{E}$, and vector potential $\boldsymbol{A}$ (defined by $\nabla \times \boldsymbol{A} = \boldsymbol{B}$, $\nabla \cdot \boldsymbol{A} = 0$, $\langle \boldsymbol{A} \rangle_r = 0$) have only one component pointing along the azimuthal direction; thus $\boldsymbol{A} = A(r,y)\,\widehat{\phi}$, $\boldsymbol{E} = E(r,y)\,\widehat{\phi}$, and $\boldsymbol{J} = J(r,y)\,\widehat{\phi}$. The vector potential of the applied field $\boldsymbol{B}_a = B_a\,\widehat{y}$ is $A_a = -(r/2)B_a$. Because $\nabla \times \boldsymbol{A} = \boldsymbol{B}$, and $\nabla \times \boldsymbol{B} = \mu_0 \boldsymbol{J}$ (here we describe the superconductor as $\boldsymbol{B} = \mu_0 \boldsymbol{H}$), we have $\mu_0 J = -\nabla^2 A = -\nabla^2 (A - A_a)$ because $\nabla^2 A_a = 0$. The solution of this Laplace equation in cylindrical geometry is

$$A(r) = -\mu_0 \int_0^a dr' \int_0^b dy' \mathcal{Q}(r,r') J(r') - \frac{r}{2} B_a, \quad (1)$$

with $\boldsymbol{r} = (r,y)$ and $\boldsymbol{r}' = (r',y')$. The integral kernel

$$\mathcal{Q}(\boldsymbol{r},\boldsymbol{r}') = f(r,r',y-y') + f(r,r',y+y'), \quad (2)$$

with

$$f(r,r',\eta) = \int_0^\pi \frac{d\phi}{2\pi} \frac{-r'\cos\phi}{(\eta^2 + r^2 + r'^2 - 2rr'\cos\phi)^{1/2}}, \quad (3)$$

is obtained by integrating the three dimensional Green function of the Laplace equation, $1/(4\pi|\boldsymbol{r}_3 - \boldsymbol{r}_3'|)$ with $\boldsymbol{r}_3 = (x,y,z)$, over the angle $\phi = \arctan(z/x)$.

To obtain the equation for $J(r,y,t)$, we express the induction law $\nabla \times \boldsymbol{E} = -\dot{\boldsymbol{B}} = -\nabla \times \dot{\boldsymbol{A}}$ in the form $E = -\dot{A}$. The gauge of $\boldsymbol{A}$, to which an arbitrary curl-free vector field may be

added, presents no problem in this simple geometry. Eliminating A from (1), one obtains

$$E[J(\boldsymbol{r},\boldsymbol{t})] = \mu_0 \int_S d^2r' \mathcal{Q}(\boldsymbol{r},\boldsymbol{r}')\dot{\boldsymbol{J}}(\boldsymbol{r}',t) - \frac{r}{2}\dot{B}_a(t), \quad (4)$$

The equation of motion for the current density can be obtained by inverting (4) as

$$\dot{J}(\boldsymbol{r},t) = \mu_0^{-1} \int_0^a dr' \int_0^b dy' \mathcal{Q}^{-1}(\boldsymbol{r},\boldsymbol{r}') \left[E(J) - \frac{r'}{2}\dot{\boldsymbol{B}}_a\right], \quad (5)$$

where $\mathcal{Q}^{-1}$ is the reciprocal kernel defined by

$$\int_0^a dr' \int_0^b dy' \mathcal{Q}^{-1}(\boldsymbol{r},\boldsymbol{r}')\mathcal{Q}(\boldsymbol{r}',\boldsymbol{r}'') = \delta(\boldsymbol{r}-\boldsymbol{r}''). \quad (6)$$

The superconducting disk is characterized by a power law $E(J)$ relationship, $E(J) = \rho J$, with

$$\rho = \rho_{\text{ff}} \left(\frac{J}{J_c}\right)^{\sigma} \quad \rho_{\text{ff}} = \rho_n \frac{B}{B_{c2}} \quad (7)$$

where ρ_{ff} is the flux flow resistivity, J_c the critical current density, ρ_n the normal state resistivity, B_{c2} the upper critical field, and $\sigma = n - 1 = U_0/kT$, U_0 represents the pinning potential, k the Boltzmann constant and T the temperature. With (7), we consider actually only the flux creep regime, the extension to flux flow regime will be considered elsewhere.

In order to show the temperature dependence of the AC susceptibility, the temperature dependence of the parameters are chosen as [14]

$$\begin{aligned} J_c &= J_{c0}(1-t^2)^{5/2}(1+t^2)^{1/2} \\ U_0 &= U_{00}(1-t^4) \\ B_{c2} &= B_{c20}\frac{1-t^2}{1+t^2} \\ \rho_n &= \rho_{n0}(t+2) \end{aligned}$$

where $t = T/T_c$, and T_c is the critical temperature.

At each temperature t, (5) is easily time integrated by starting with $J(r,y,t=0) = 0$ at time $t = 0$ and then putting $J(r,y,t=t+dt) = J(r,y,t) + \dot{J}(r,y,t)dt$. The vector potential can then be derived from (1) and the magnetic field $\boldsymbol{B} = \nabla \times \boldsymbol{A}$. The magnetic moment can be obtained by integrating the current density over the sample volume V as

$$\boldsymbol{m} = \frac{1}{2}\int_V \boldsymbol{r} \times \boldsymbol{J}(\boldsymbol{r}) d^3r. \quad (8)$$

For sinusoidal $H(t) = H_{\text{ac}}\sin(\omega t)$, one may define the nonlinear complex AC susceptibilities $\chi_\mu = \chi'_\mu - i\chi''_\mu$, $\mu = 1,2,3,\ldots$

$$\chi_\mu = \frac{i}{\pi H_{\text{ac}}} \int_0^{2\pi} m(t) e^{-i\mu\omega t} d(\omega t). \quad (9)$$

Usually, the χ_μ are normalized such that for $H_{\text{ac}} \to 0$ or $\omega \to \infty$ the ideally diamagnetic susceptibility $\chi(0,\omega)$ results; this normalization is achieved by dividing all χ_μ by the magnitude of the initial slope $|m'(0)| = \lim_{H_a \to 0} |\partial m(H_a)/\partial H_a|$. In this paper only the fundamental susceptibility ($\mu = 1$) will be considered, denoting χ_1 by χ. For all the calculations, we use a reduced unit of $\mu_0 = a = \rho_{n0} = J_{c0} = 1$, H, B, t, ω and J are in units of $J_{c0}a$, $\mu_0 J_{c0}a$, $\mu_0 a/\rho_{n0}$, $\rho_{n0}/\mu_0 a$ and J_{c0}, respectively.

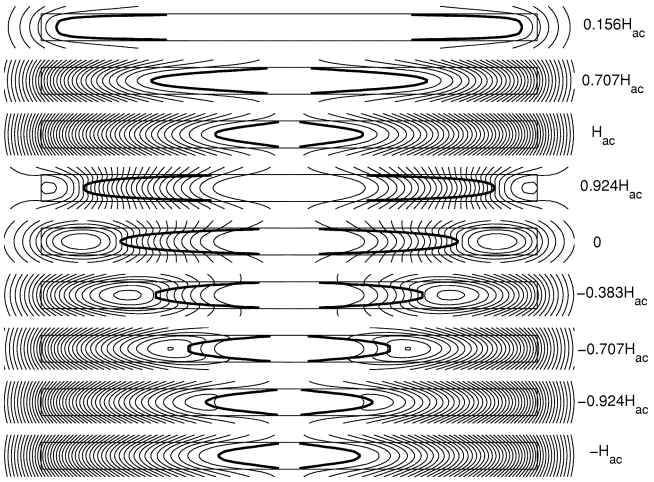

Fig. 1. Magnetic field lines (solid lines) and flux fronts (dashed lines) when the applied field changes from 0 to H_{ac} to $-H_{\text{ac}}$ for a disk with side ratio $b/a = 0.1$, $\sigma = 50$, $H_{\text{ac}} = 1e-3$, and ωB_{c20}, at $t = 0.92$.

III. Results and Discussions

Fig. 1 shows the magnetic field lines and the flux fronts of a superconducting disk with side ratio $b/a = 0.1$, $\sigma = 50$, $H_{\text{ac}} = 1e-3$, and $\omega B_{c20} = 1$, at $t = 0.92$, for flux penetration and exit as the applied field changes from 0 to H_{ac} and to $-H_{\text{ac}}$. $t = 0.92$ is the temperature at which the imaginary part of the AC susceptibility χ'' reaches the maximum. However, as can be seen from Fig. 1, the flux fronts are not closed when $H(t)$ reaches H_{ac}. For an infinite long cylinder under perpendicular magnetic field, χ'' reaches a maximum as the flux fronts meet at the center of the sample, and the current density can then be calculated by $J = H_{\text{ac}}/d$, where d is the radius of the cylinder. However, for a finite disk under perpendicular magnetic field, this simple relationship between H_{ac} and J is not valid any more, and one has to consider the curvature of the magnetic flux lines except when a very high DC field is applied. The flux fronts are calculated most conveniently as the two contour lines where the current density J equals $\pm J_c/2$ for increasing field and equals 0 for decreasing field [19]–[24].

For local relaxation measurement [25], [26], in which hall probes are placed onto the surface of a sample perpendicular to the magnetic field, the current density is usually approximately calculated using the perpendicular component of the field (B_y in Fig. 1) and B_r is neglected. This may result in some uncertainties as can be seen from Fig. 1, both B_y and B_r contribute to the current density. As the side ratio b/a increases, the curvature becomes less and less important, and the parallel limit could be a good approximation, see Fig. 2.

Fig. 3 shows the calculated AC susceptibility versus temperature for a superconducting disk with side ratio $b/a = 0.1$, creep exponent $\sigma = 50$, AC field amplitude $H_{\text{ac}} = 1e-3$, for different AC field frequencies. As the frequencies decreases, the transition temperature shifts to lower value, the peak height in χ'' decreases and the breadth in χ'' increases as it moves to

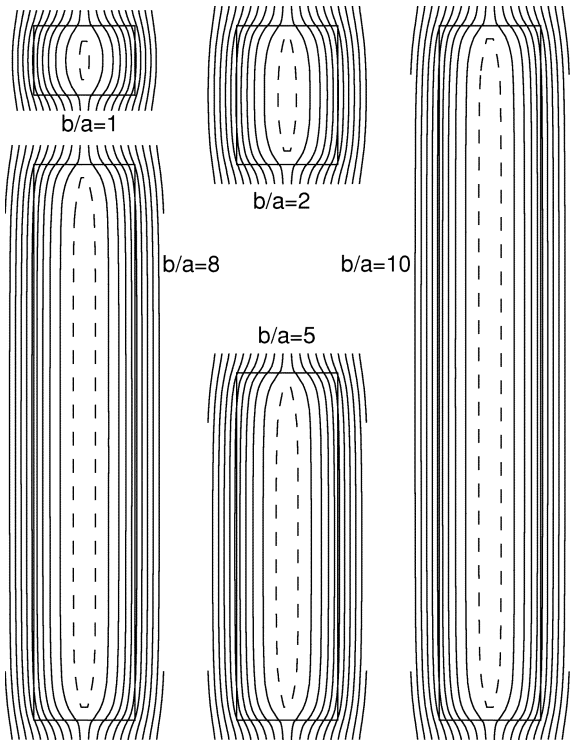

Fig. 2. Magnetic field lines (solid lines) and flux fronts (dashed lines) at $H(t) = H_{\rm ac}$ for disks with side ratios $b/a = 1$, 2, 5, 8, 10, $\sigma = 50$, $H_{\rm ac} = 1e-3$, and $\omega B_{c20} = 1$, at $t = 0.96$.

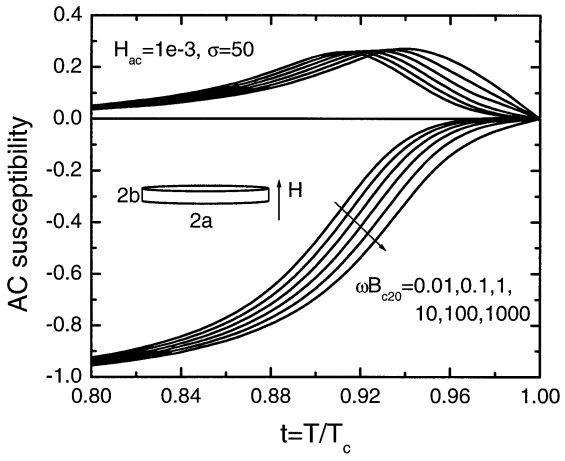

Fig. 3. AC susceptibility versus temperature for a superconducting disk with side ratio $b/a = 0.1$, creep exponent $\sigma = 50$, AC field amplitude $H_{\rm ac} = 1e-3$, for different AC field frequencies indicated in the figure.

lower temperature, which is in good agreement with experimental data [13]. The features shown here are similar to what have been obtained for a slab under parallel field $B_{\rm dc} \gg B_{\rm ac}$ [14].

In Fig. 4, we plot the calculated curves of χ' and χ'' as a function of temperature at various ac field amplitudes, for a superconducting disk with side ratio $b/a = 0.1$, creep exponent $\sigma = 50$ and AC field frequency $\omega B_{c20} = 1$. As $H_{\rm ac}$ increases, the height of the peak in χ'' decreases, while the breadth in χ'' increases as it moves to lower temperature. Experimentally, it has been observed that when $B_{\rm dc} \gg B_{\rm ac}$ is satisfied, the height of the peak in χ'' increases as $H_{\rm ac}$ increases [11]. In this paper,

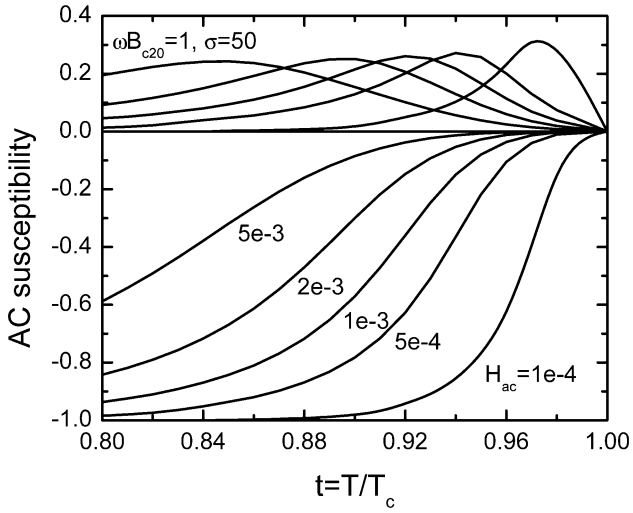

Fig. 4. AC susceptibility versus temperature for a superconducting disk with side ratio $b/a = 0.1$, creep exponent $\sigma = 50$, AC field frequencies $\omega B_{c20} = 1$, for different AC field amplitudes indicated in the figure.

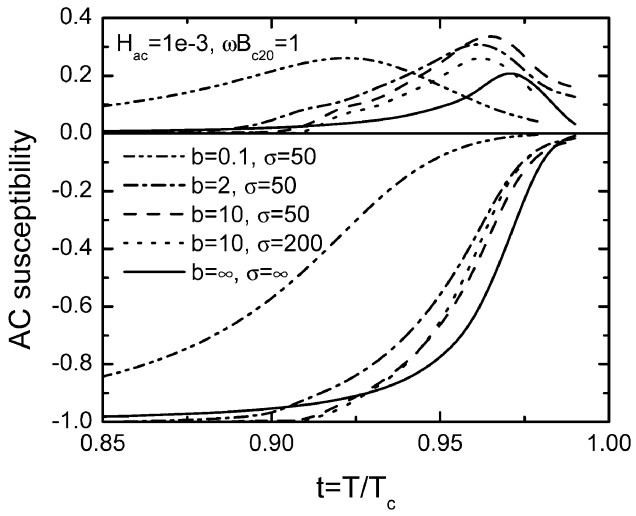

Fig. 5. AC susceptibility versus temperature for superconducting disks with different side ratio s and creep exponents indicated in the figure, at AC field frequencies $\omega B_{c20} = 1$ and AC field amplitude $H_{\rm ac} = 1e-3$.

all the calculations are conducted without DC field, it is expected that the AC field may have the same effect as that of the DC magnetic field. Usually, increasing $B_{\rm dc}$ results in lower height and larger breadth in χ'', as has been demonstrated by both calculation and experiment [14], [11]

Fig. 5 shows the AC susceptibility as a function of temperature for superconducting disks with different side ratios $b/a =$ 0.1, 2, 10, ∞ and creep exponents $\sigma =$ 50,200, ∞ for AC field amplitude $H_{\rm ac} = 1e-3$ and frequency $\omega B_{c20} = 1$. As the side ratio increases, the peak in χ'' shifts to higher temperature with higher peak height, whereas increasing the creep exponent σ results in lower peak height and higher transition. With increasing side ratio and creep exponent, the ac susceptibility goes to the limit of the solid line ($b/a = \infty$, $\sigma = \infty$) which shows the Bean critical state limit for an infinite long cylinder under parallel magnetic field. It should be noted that the critical state model predicts a constant height in χ'' independent of the AC

field amplitude and frequency and therefore cannot explain the features shown in Figs. 3–5. The effects of the side ratio on the calculation of pinning potential using ac susceptibility will be discussed elsewhere.

IV. Conclusion

The temperature dependent complex AC susceptibilities of high temperature superconducting disks ($E(j) = E_0(j/j_c)^n$ and $B = \mu_0 H$) in perpendicular AC fields (in absence of DC magnetic field) have been calculated from first principles. The field profiles and the current distribution in the disks have been derived, which demonstrate many features different from what have been observed in the configuration of infinite long cylinders or slabs under parallel field. The curvature of the magnetic field lines caused by the finite thickness of the sample has been shown to have obvious effects on the AC susceptibility. The calculated temperature dependent AC susceptibilities for different AC field amplitudes, frequencies, pinning potential, and sample thickness have been obtained and the characteristics have been discussed. The results of such a realistic configuration of finite-thickness samples in perpendicular fields can be compared directly to the experimental results.

References

[1] P. Seng, R. Gross, U. Baier, M. Rupp, D. Koelle, R. P. Hue-bener, P. Schmitt, G. Saemann-Ischenko, and L. Schultz, *Physica C*, vol. 192, p. 403, 1992.
[2] C. P. Bean, *Rev. Mod. Phys.*, vol. 2, p. 31, 1964.
[3] J. I. Gittleman and B. Rosenblum, *Phys. Rev. Lett.*, vol. 16, p. 734, 1991.
[4] A. M. Campbell, *J. Phys. C*, vol. 2, p. 1492, 1969.
[5] ——, *J. Phys. C*, vol. 4, p. 3186, 1971.
[6] A. P. Malozemoff, T. K. Worthington, Y. Yeshurun, F. Holtzberg, and P. H. Kes, *Phys. Rev. B*, vol. 38, p. 7203, 1988.
[7] J. van den Berg, C. J. van der Beek, P. H. Kes, J. A. Mydosh, M. J. V. Menken, and A. A. Menovsky, *Supercond. Sci. Technol.*, vol. 1, p. 242, 1989.
[8] A. Gupta, P. Esquinazi, H. F. Braun, and H. W. Neumüller, *Europhys. Lett.*, vol. 10, p. 663, 1989.
[9] P. L. Gammel, *J. Appl. Phys.*, vol. 67, p. 4676, 1990.
[10] J. H. P. M. Emmen, G. M. Stollman, and W. J. M. de Jonge, *Physica C*, vol. 169, p. 418, 1990.
[11] T. Ishida and R. B. Goldfarb, *Phys. Rev. B*, vol. 41, p. 8937, 1990.
[12] C. J. van der Beek and P. H. Kes, *Phys. Rev. B*, vol. 43, p. 13 032, 1991.
[13] F. Gömöry and T. Takács, *Physica C*, vol. 217, p. 297, 1993.
[14] M. J. Qin and X. X. Yao, *Phys. Rev. B*, vol. 54, p. 7536, 1996.
[15] M. J. Qin and C. K. Ong, *Phys. Rev. B*, vol. 61, p. 9786, 2000.
[16] M. J. Qin, S. Y. Ding, C. Ren, X. X. Yao, Y. X. Fu, C. B. Cai, T. S. Shi, and G. Y. Wang, *Physica C*, vol. 262, p. 127, 1996.
[17] S. Y. Ding, G. Q. Wang, X. X. Yao, H. T. Peng, Q. Y. Peng, and S. H. Zhou, *Phys. Rev. B*, vol. 51, p. 9107, 1995.
[18] C. J. van der Beek, V. B. Geshkenbein, and V. M. Vinokur, *Phys. Rev. B*, vol. 48, p. 3393, 1993.
[19] E. H. Brandt, *Phys. Rev. B*, vol. 58, p. 6506, 1998.
[20] ——, *Phys. Rev. B*, vol. 58, p. 6523, 1998.
[21] ——, *Phys. Rev. B*, vol. 54, p. 4246, 1996.
[22] ——, *Phys. Rev. B*, vol. 60, p. 11939, 1999.
[23] ——, *Phys. Rev. B*, vol. 59, p. 3369, 1999.
[24] ——, *Phys. Rev. B*, vol. 55, p. 14513, 1997.
[25] D. Giller, A. Shaulov, R. Prozorov, Y. Abulafia, Y. Wolfus, L. Burlachkov, Y. Yeshurun, E. Zeldov, V. M. Vinokur, J. L. Peng, and R. L. Greene, *Phys. Rev. Lett.*, vol. 79, p. 2542, 1997.
[26] Y. Abulafia, A. Shaulov, Y. Wolfus, R. Prozorov, L. Burlachkov, Y. Yeshurun, D. Majer, E. Zeldov, and V. M. Vinokur, *Phys. Rev. Lett.*, vol. 75, p. 2404, 1995.